Dimensionality dependence of aging in kinetics of diffusive phase separation: Behavior of order-parameter autocorrelation

Jiarul Midya, Suman Majumder, and Subir K. Das*

Theoretical Sciences Unit, Jawaharlal Nehru Centre for Advanced Scientific Research, Jakkur P.O., Bangalore 560064, India

(Received 18 December 2014; published 17 August 2015)

Behavior of two-time autocorrelation during the phase separation in solid binary mixtures is studied via numerical solutions of the Cahn-Hilliard equation as well as Monte Carlo simulations of the Ising model. Results are analyzed via state-of-the-art methods, including the finite-size scaling technique. Full forms of the autocorrelation in space dimensions 2 and 3 are obtained empirically. The long-time behavior is found to be power law, with exponents unexpectedly higher than the ones for the ferromagnetic ordering. Both Cahn-Hilliard and Ising models provide consistent results.

DOI: 10.1103/PhysRevE.92.022124 PACS number(s): 05.70.Ln, 05.70.Fh, 81.40.Cd

I. INTRODUCTION

Understanding of aging phenomena in out-of-equilibrium systems, except for special situations like steady state, is of fundamental importance [1]. There have been serious activities on this issue concerning living [2,3] as well as nonliving matters, especially in problems related to domain growth [1,4–14] and glassy dynamics [15–19]. Among other quantities, aging phenomena is studied via the two-time autocorrelation function [4],

$$C(t,t_w) = \langle \psi(\vec{r},t)\psi(\vec{r},t_w)\rangle - \langle \psi(\vec{r},t)\rangle\langle \psi(\vec{r},t_w)\rangle, \quad (1)$$

where ψ is a space ($\vec{r}$) and time-dependent order parameter, t_w is the waiting time or age of the system, t ($>t_w$) is the observation time, and the angular brackets represent statistical averaging over space and initial configurations.

In phase-ordering systems [20], though time translation invariance is broken, $C(t,t_w)$ is expected to exhibit scaling with respect to t/t_w. Important examples are ordering of spins in a ferromagnet, kinetics of phase separation in a binary ($A+B$) mixture, etc., having been quenched to a temperature (T) below the critical value (T_c), from a homogeneous configuration. Though full forms are unknown even for very simple models, asymptotically ($t/t_w \to \infty$) $C(t,t_w)$ is expected to obey power-law scaling behavior as [4,6]

$$C(t,t_w) \sim x^{-\lambda}; x = \ell/\ell_w. \quad (2)$$

In Eq. (2), ℓ and ℓ_w are the average sizes of domains, formed by spins or particles of similar type, at times t and t_w, respectively. Typically ℓ and t are related to each other via power laws.

For nonconserved order-parameter dynamics, e.g., ordering in a ferromagnet, such scaling has been observed and the values of the exponent λ have been accurately estimated [6,14] in different space dimensions d. There the exponents follow the bounds

$$d/2 \leqslant \lambda \leqslant d, \quad (3)$$

predicted by Fisher and Huse (FH) [4]. In kinetics of phase separation in solid mixtures, for which the order parameter is a conserved quantity, the state of understanding is far from satisfactory, due to various difficulties. There, values of λ remain unknown, except for lower bounds discussed below.

Yeung *et al.* [7] put a more general lower bound on λ as

$$\lambda \geqslant \frac{(\beta+d)}{2}, \quad (4)$$

where β is the exponent for small wave-vector power-law enhancement of equal-time structure factor, which, depending upon the dynamics, becomes important for $t_w \gg 1$, as stated below. In nonconserved dynamics, $\beta = 0$ and so the FH lower bound is recovered. For conserved order parameter dynamics, on the other hand, $\beta = 4$ in both $d = 2$ and 3 at late time. Thus, the FH upper bound is violated. Simulations of the Cahn-Hilliard (CH) equation [20],

$$\frac{\partial \psi(\vec{r},t)}{\partial t} = -\nabla^2[\psi(\vec{r},t) + \nabla^2\psi(\vec{r},t) - \psi^3(\vec{r},t)], \quad (5)$$

by Yeung *et al.* [7], observed $\lambda > 3$ in $d = 2$, consistent with their bound. From these simulations, the authors, however, did not accurately quantify λ; scaling of $C(t,t_w)$ with respect to t/t_w was not demonstrated; focus was rather on the sensitivity of the aging dynamics to the correlations in the initial configurations. Situation is far worse in $d = 3$, with respect to the CH equation as well as the Ising model [1,20],

$$H = -J\sum_{\langle ij\rangle} S_i S_j; S_i = \pm 1; J > 0. \quad (6)$$

In this paper, we study both CH equation and the Ising model, used for understanding diffusive phase separation as in solid mixtures, in $d = 2$ (on regular square lattice) and $d = 3$ (on simple cubic lattice), via extensive simulations, to quantify the decay of $C(t,t_w)$. We observe scaling of $C(t,t_w)$ with respect to x, which tends to a power law for large x. Via computations of the instantaneous exponent [21–23],

$$\lambda_i = -\frac{d\ln[C(t,t_w)]}{d\ln x}, \quad (7)$$

and application of the finite-size scaling technique [24,25], we find that $\lambda \simeq 3.6$ in $d = 2$ and $\simeq 7.5$ in $d = 3$. Though these numbers respect the bounds of Yeung *et al.* [7], the high value in $d = 3$ is surprising. Furthermore, a general form for the full scaling functions has been obtained empirically.

The rest of the paper is organized as follows. We describe the methodology in Sec. II. Results are presented in Sec. III.

*das@jncasr.ac.in

Finally, Sec. IV concludes the paper with a brief summary and discussion.

II. METHODS

We numerically solve the CH equations on a regular lattice, via Euler discretization method. With the Ising model, phase-separation kinetics in a solid binary mixture is studied via the Kawasaki exchange Monte Carlo (MC) [25] simulations, to be referred to as KIM. An up-spin ($S_i = +1$), for this problem, may correspond to an A particle and a down-spin (-1) to a B particle. In this MC scheme, one randomly chooses a pair of nearest-neighbor spins and tries their position exchange. The moves are accepted according to standard Metropolis algorithm [25]. Due to the coarse-grained nature of the CH equation, as opposed to the atomistic Ising model, one can explore large effective length in simulations. The order parameter in CH equation corresponds to a coarse-graining [26] of the Ising spins, typically over the equilibrium correlation length ξ. Then, a positive value of ψ means an A-rich region and for a B-rich region, ψ will have a negative number. For the calculation of $C(t,t_w)$, we have used hardened configurations with numbers $+1$ and -1, for the order parameter, for both the models. In the CH equation, a noise term is intentionally omitted to investigate if there is any strong effect of the latter, since in the KIM it is automatically included. However, within the accuracy of the simulations, we do not observe any significant difference between the CH model and the KIM results.

The average domain length, ℓ, was measured from the first moment of domain-size distribution, $P(\ell_d,t)$, as [23]

$$\ell = \int \ell_d P(\ell_d,t) d\ell_d, \tag{8}$$

where ℓ_d is the distance between two successive domain boundaries in any direction. Throughout the paper, all lengths are presented in units of the lattice constant a. In MC simulations, time is counted in units of Monte Carlo steps (MCS), each MCS consisting of L^d trial moves, where L is the linear dimension of a periodic square or cubic system. In CH equation, t is expressed in dimensionless units [27]. All results, for both the models, are presented after averaging over at least 50 initial realizations, for quenches from random configurations, mimicking $T = \infty$, to $T = 0.6T_c$. Such value, instead of 0, of T was chosen to avoid metastability that is often encountered in conserved dynamics at low T.

III. RESULTS

In Fig. 1(a), we present the plots of $C(t,t_w)$, versus x, for different values of t_w, from the solutions of CH model in $d = 2$. As seen, one needs large enough value of t_w to observe appropriate scaling behavior (collapse of data), compared to ordering in ferromagnets [14]. In the case of Ising ferromagnet in $d = 2$, the scaling is observed from $t \simeq 10$ MCS. It appears that late occurrence of scaling in conserved dynamics is due to slow domain growth. Our observation from Ising model suggests, scaling is achieved from $\ell_w \simeq 10$ lattice constants, irrespective of conservation of the order parameter. Between the two data sets with largest values of t_w, the deviation from

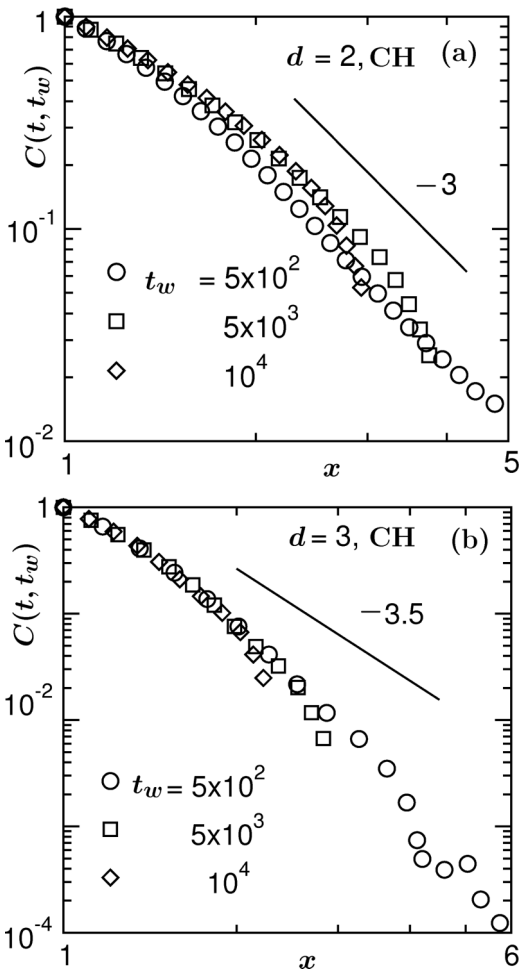

FIG. 1. (a) Autocorrelation function, $C(t,t_w)$, from the $d = 2$ Cahn-Hilliard (CH) model, are plotted vs. x ($=\ell/\ell_w$), for different values of t_w. The solid line there corresponds to a power-law decay with exponent 3. (b) Same as (a) but for the $d = 3$ CH model. The solid line there has a power-law decay exponent 3.5. The system sizes used are $L = 256$ ($d = 2$) and 200 ($d = 3$).

each other, for large x, is due to the finite-size effects. Similar plots for the $d = 3$ CH model are presented in Fig. 1(b). Here we have chosen t_w values from the scaling regime only. Compared to $d = 2$, scaling in $d = 3$ starts earlier because of the fact that the domain growth amplitude is larger in the latter dimension. Again, deviation from the master curve, starting at different values of x for different t_w, are primarily related to the finite-size effects. In both Figs. 1(a) and 1(b), the system sizes are kept fixed, only the values of t_w are varied. A similar observation, with respect to the above-mentioned deviation for different choices of t_w, can be made, when, for same value of t_w, data are presented for different system sizes.

In the scaling parts, both in Figs. 1(a) and 1(b), continuous bending is observable, in these log-log plots. Thus, power laws, if they exist, carry corrections. The solid lines in these figures are power-law decays with exponents 3 and 3.5, respectively, corresponding to the bounds of Yeung *et al.* [7]. For large x, simulation data in $d = 2$ appear reasonably consistent with the bound. The asymptotic exponent, in $d = 3$, on the other hand, appear much higher than 3.5.

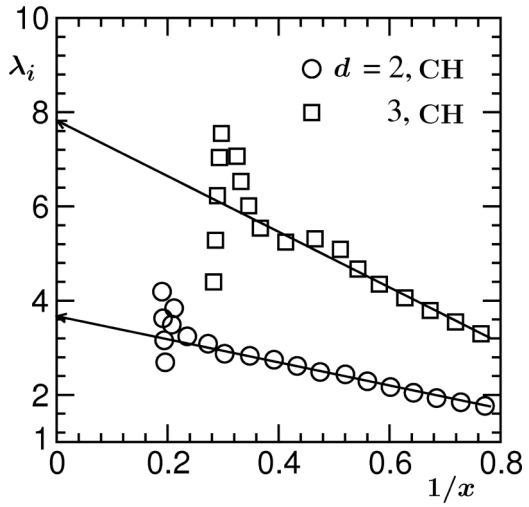

FIG. 2. Instantaneous exponents λ_i are plotted vs. $1/x$. Results are shown only from the solutions of the CH equations, in both $d = 2$ and 3. The solid lines are guides to the eye. The $d = 2$ data are for $t_w = 5 \times 10^3$ with $L = 400$. In $d = 3$ the numbers are 10^3 and 200.

With the expectation that power laws indeed exist asymptotically, in Fig. 2 we present plots of instantaneous exponents [6,14,21–23] λ_i, for both $d = 2$ and 3, versus $1/x$. In addition to providing λ, from the extrapolations to $x = \infty$, such exercise may be useful for obtaining crucial information on the full forms of $C(t,t_w)$. For $d = 2$, the data are obtained for $t_w = 5 \times 10^3$, and for $d = 3$, the data correspond to $t_w = 10^3$. In both cases, the results appear reasonably linear [6,14]. The solid lines there are extrapolations to $x = \infty$, accepting the linear trends. These indicate $\lambda \simeq 3.60$ in $d = 2$ and $\simeq 7.80$ in $d = 3$. Again, while the value in $d = 2$ is consistent and close to the bound of Yeung *et al.* [7], the observation of surprisingly high number in $d = 3$ is certainly interesting. We intend to obtain more accurate values via appropriate finite-size scaling analyses [24,25]. This is considering the fact that the choice of the regions in Fig. 2, for performing least-square fitting, is not unambiguous due to finite-size effects and strong statistical fluctuations at large x. Also, for very small x (data excluded), there is rapid decay of $C(t,t_w)$ related to the fast equilibration of domain magnetization m (being very close to unity at the chosen value of T for $d = 2$ Ising model). Here note that this latter contribution decays from $(1 - m^2)$ to 0. At this temperature (noting that critical phenomena is typically observed within 10% of T_c, we are significantly below the critical regime), thus, the time scale of this equilibration is short and so the analysis gets affected only very close to $x = 1$.

Since the corrections to the asymptotic decay laws are seen to be strong for finite x, a reasonable idea about the full forms of the decays is essential for accurate finite-size scaling analyses. Those, however, are nonexistent in the literature. Here we obtain the forms empirically. Assuming power-law behavior of the data sets in Fig. 2, we write

$$\lambda_i = \lambda - \frac{A_c}{x^\gamma}, \tag{9}$$

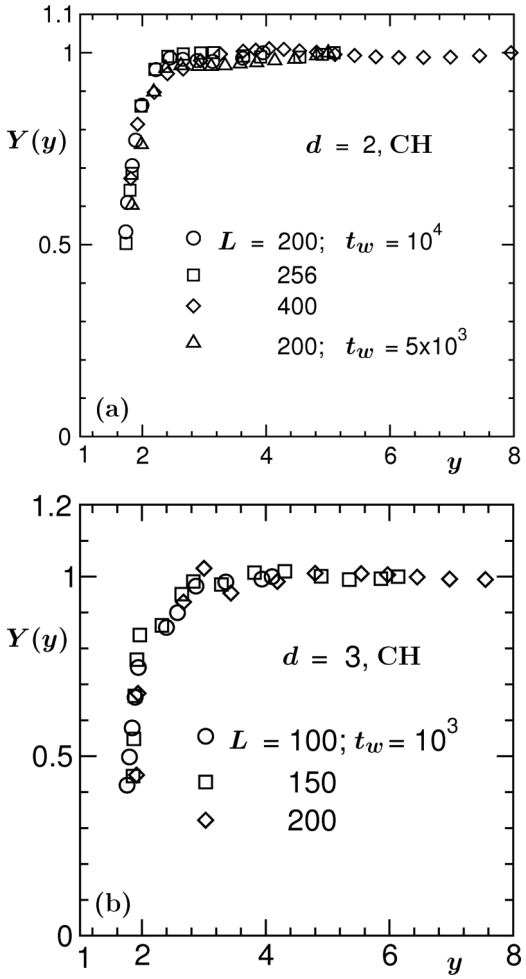

FIG. 3. (a) Finite-size scaling plot of $C(t,t_w)$ from $d = 2$ CH model. The scaling function Y is plotted vs. y, using data from different system sizes and t_w values. The optimum collapse of data, the presented one, was obtained for $\lambda = 3.47$. (b) Same as (a), but the CH model in $d = 3$. Here the value of λ is 7.30.

A_c and γ being constants. This, via Eq. (7), provides

$$C(t,t_w) = C_0 \exp\left(-\frac{A_c}{\gamma x^\gamma}\right) x^{-\lambda}, \tag{10}$$

C_0 being a constant. For finite-size scaling analysis, one needs to introduce a scaling function:

$$Y(y) = C(t,t_w) \exp\left(\frac{A_c}{\gamma x^\gamma}\right) x^\lambda; \quad y = L/\ell. \tag{11}$$

The variable y gets separated from x because of the fact that $y = \frac{L/\ell_w}{x}$ and x contains ℓ_w in the denominator. For appropriate choices of A_c, γ, and λ, one should obtain a master curve for Y, when data from different system sizes are used. If the above-mentioned factorization between x and y truly holds, we should obtain collapse of data for different values of t_w as well. We will demonstrate that this indeed is true. The behavior of Y should be flat in the finite-size unaffected region and a deviation from it will mark the onset of finite-size effects.

By examining the data in Fig. 2 [also see Fig. 4(b) for KIM], we fix γ to 1. In Fig. 3(a), we show a finite-size scaling plot for data from the $d = 2$ CH model, using different values of

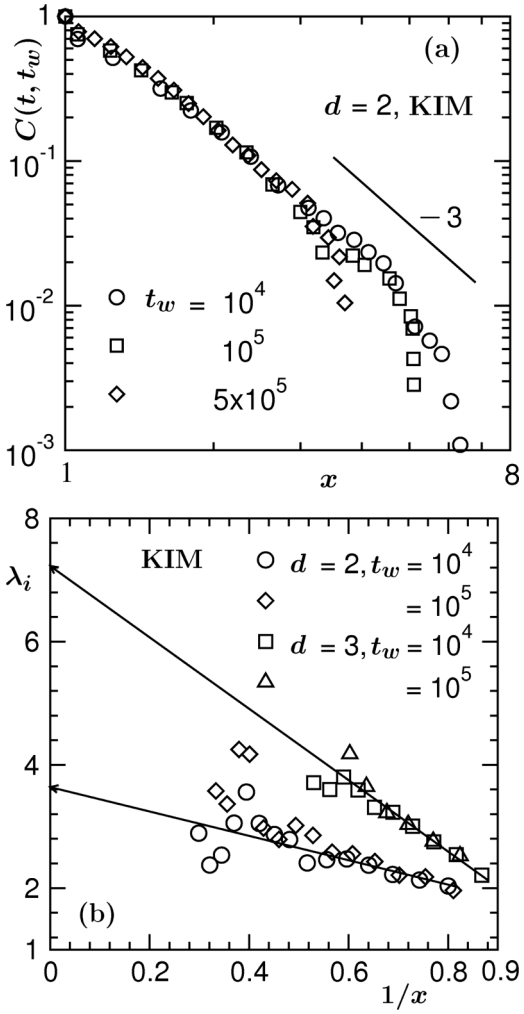

FIG. 4. (a) Same as Fig. 1(a) but for the $d = 2$ Ising model. (b) Same as Fig. 2 but for the Ising model. The oscillatory behavior of large x data in $d = 2$ is statistical fluctuation. In $d = 2$ the results are from $L = 512$, and in $d = 3$ we have used $L = 100$.

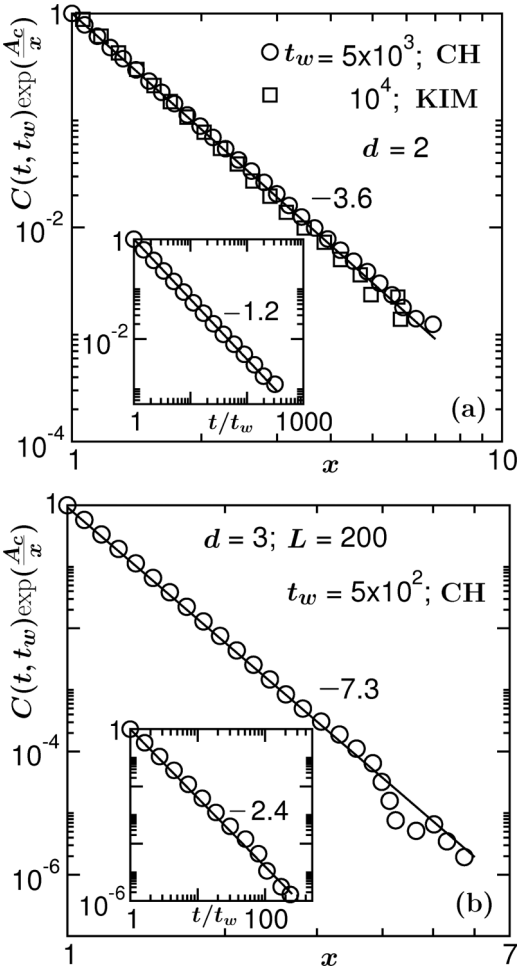

FIG. 5. (a) $C(t,t_w)\exp(A_c/x)$ is plotted vs. x, for $d = 2$, on log-log scale. Results from both KIM ($L = 512$) and CH model ($L = 1024$) are included. The solid line represents a power-law decay with $\lambda = 3.6$. The inset shows the same result vs. t/t_w, only for the CH model. The solid line there has a power-law decay with exponent 1.2. (b) Same as (a) but from $d = 3$ and only for CH model. The decay exponents for the solid lines are mentioned on the figure. In all the plots we have used the values of A_c as obtained from the finite-size scaling analyses of CH model data.

L and t_w. The presented results correspond to best collapse, obtained for $A_c = 2.25$ and $\lambda = 3.47$. The value of t_w used for different L is 10^4. For $L = 200$ we have used two different t_w values, viz., 10^4 and 5×10^3. A similar exercise for the $d = 3$ CH data is presented in Fig. 3(b). In this case we have fixed t_w and varied only L. Again, the data collapse looks quite reasonable and was obtained for $A_c = 5.1$ and $\lambda = 7.30$. The value of t_w, in this case, was set to 10^3. The reason behind choosing smaller value of t_w in $d = 3$, than in $d = 2$, is computational difficulty. It is extremely difficult to accumulate data for further decades in time, starting from very high value of t_w, particularly in $d = 3$. Nevertheless, this chosen value of t_w falls within the scaling regime. As already mentioned, for similar temperatures, amplitude of growth is larger in $d = 3$ and the scaling of $C(t,t_w)$ is related more closely to the value of ℓ_w.

We now move to present results from KIM. In Fig. 4(a) we show the autocorrelations from different values of t_w in $d = 2$, for $L = 512$. Scaling is poor for t_w below 10^4 MCS and so those results are excluded. Despite strong statistical fluctuations, it is recognizable that the decay of $C(t,t_w)$ in the latter part is on the higher side of the bound of Yeung *et al.* [7], represented by the solid line.

In Fig. 4(b) we show the instantaneous exponents for the Ising model in $d = 2$ and 3, versus $1/x$. In each dimension, we have included two values of t_w from the scaling regime. While results for different t_ws, in a particular dimension, are consistent with each other, finite-size effects appear earlier for larger value of t_w, as expected. Thus, for extrapolations to $x = \infty$, data sets with smaller t_w are used. This exercise provides $\lambda \simeq 3.60$ and $\simeq 7.30$ in $d = 2$ and 3, respectively. These values are in agreement with the ones obtained for the CH model via various methods of analysis.

In Fig. 5(a) we show plots of $C(t,t_w)\exp(A_c/x)$, from $d = 2$, on log-log scale, versus x $(=\ell/\ell_w)$. The results from KIM and CH models are consistent with each other and obey power law with $\lambda = 3.6$, represented by the solid line. For

the CH model, the value of L here is much larger than the previous figures. This value of L was used with the objective of confirming the finite-size scaling conclusions (from relatively smaller systems) via brute force method. Given that the scaling starts for large t_w, range of x is significant. As shown in the inset, the CH model results span several decades in t/t_w. In this connection we mention that the longest run lengths (associated with largest systems) for the CH model are $t = 2 \times 10^6$ and 2×10^5 in $d = 2$ and 3, respectively; for the Ising model these numbers are 5×10^7 and 4×10^6. To the best of our knowledge, the quoted numbers are orders of magnitude larger than any previous simulations that used conventional simulation methods for this purpose. Since the objective here has been to access long time scales so that the scaling behavior can be proved, it was necessary to work with slightly smaller systems. Figure 5 verifies that the conclusions drawn from the finite-size scaling analyses, involving smaller systems, indeed are appropriate. The exponents for the power-law decays in the main frame and the inset are consistent with each other, given that $\alpha = 1/3$. Analogous results from $d = 3$ CH model are shown in the Fig. 5(b). In both Figs. 5(a) and 5(b), we have used the earliest available values of t_w for which scaling is observed. This helps exploring reasonably large range for x, without encountering finite-size effects, i.e., ℓ being significantly smaller than L. In Fig. 5(a), e.g., data for more than two decades in t/t_w (for both the models) correspond to $L/\ell > 5$. This picture holds for more than a decade in t/t_w in Fig. 5(b). We note here, recently it was convincingly demonstrated [23] that finite-size effects in conserved order-parameter dynamics appear only when ℓ is as large as 3/4 of the equilibrium limit. Thus, results presented in Fig. 5 are free from finite-size effects.

IV. CONCLUSION

We have studied aging dynamics for the phase separation in solid binary mixtures via Cahn-Hilliard and Ising models. Results for the two-time autocorrelation, $C(t,t_w)$, are presented from simulations in both $d = 2$ and 3. Decays of $C(t,t_w)$ appear power law in large x limit. The exponents for these power laws were obtained via various different analyses, including finite-size scaling. For the finite-size scaling analysis, full forms of the autocorrelations were essential, which we obtained empirically. All these methods provide consistent values of the decay exponent λ for different models. These are $\lambda \simeq 3.6$ in $d = 2$ and $\lambda \simeq 7.5$ in $d = 3$, within 5% error. To construct a dimension-dependent expression for λ, involving d and β, from this kind of analyses, one needs to study the phenomena in more dimensions. In this context, in $d = 1$ one should exercise the caution that β (= 2) has a different value [28].

ACKNOWLEDGMENTS

The authors acknowledge financial support from Department of Science and Technology, India, via Grant No. SR/S2/RJN-13/2009. J.M. is grateful to UGC, India, for research fellowship, and S.M. acknowledges JNCASR for the same. S.K.D. is thankful to the Marie Curie Actions Plan of European Commission (FP7-PROPLE-2013-IRSES Grant No. 612707, DIONICOS) for partial financial support.

[1] *Kinetics of Phase Transitions*, edited by S. Puri and V. Wadhawan (CRC Press, Boca Raton, 2009).
[2] R. M. Zorzenon dos Santos and A. T. Bernardes, Phys. Rev. Lett. **81**, 3034 (1998).
[3] M. Costa, A. L. Goldberger, and C.-K. Peng, Phys. Rev. Lett. **95**, 198102 (2005).
[4] D. S. Fisher and D. A. Huse, Phys. Rev. B **38**, 373 (1988).
[5] G. F. Mazenko, Phys. Rev. B **42**, 4487 (1990).
[6] F. Liu and G. F. Mazenko, Phys. Rev. B **44**, 9185 (1991).
[7] C. Yeung, M. Rao, and R. C. Desai, Phys. Rev. E **53**, 3073 (1996).
[8] G. F. Mazenko, Phys. Rev. E **69**, 016114 (2004).
[9] J. F. Marko and G. T. Barkema, Phys. Rev. E **52**, 2522 (1995).
[10] S. Puri and D. Kumar, Phys. Rev. Lett. **93**, 025701 (2004).
[11] S. van Gemmert, G. T. Barkema, and S. Puri, Phys. Rev. E **72**, 046131 (2005).
[12] S. Ahmad, F. Corberi, S. K. Das, E. Lippiello, S. Puri, and M. Zannetti, Phys. Rev. E **86**, 061129 (2012).
[13] S. Majumder and S. K. Das, Phys. Rev. Lett. **111**, 055503 (2013).
[14] J. Midya, S. Majumder, and S. K. Das, J. Phys.: Condens. Matter **26**, 452202 (2014).
[15] B. Abou and F. Gallet, Phys. Rev. Lett. **93**, 160603 (2004).
[16] G. G. Kenning, G. F. Rodriguez, and R. Orbach, Phys. Rev. Lett. **97**, 057201 (2006).
[17] L. Berthier, Phys. Rev. Lett. **98**, 220601 (2007).
[18] E. Bouchbinder and J. S. Langer, Phys. Rev. E **83**, 061503 (2011).
[19] J. Bergli and Y. M. Galperin, Phys. Rev. B **85**, 214202 (2012).
[20] A. J. Bray, Adv. Phys. **51**, 481 (2002).
[21] D. A. Huse, Phys. Rev. B **34**, 7845 (1986).
[22] J. G. Amar, F. E. Sullivan, and R. D. Mountain, Phys. Rev. B **37**, 196 (1988).
[23] S. Majumder and S. K. Das, Phys. Rev. E **81**, 050102 (2010).
[24] M. E. Fisher, in *Critical Phenomena*, edited by M. S. Green (Academic Press, London, 1971).
[25] D. P. Landau and K. Binder, *A Guide to Monte Carlo Simulations in Statistical Physics*, 3rd ed. (Cambridge University Press, Cambridge, 2009).
[26] A. Onuki, *Phase Transition Dynamics* (Cambridge University Press, Cambridge, 2002).
[27] K. Binder, S. Puri, S. K. Das, and J. Horbach, J. Stat. Phys. **138**, 51 (2010).
[28] S. N. Majumdar, D. A. Huse, and B. D. Lubachevsky, Phys. Rev. Lett. **73**, 182 (1994).